

Article

Rigid Polyurethane Foams Modified with Soybean-Husk-Derived Ash as Potential Insulating Materials

Anna Magiera ¹, Monika Kuźnia ¹, Aleksandra Błoniarz ² and Aneta Magdziarz ^{1,*}

¹ Department of Heat Engineering and Environment Protection, Faculty of Metals Engineering and Industrial Computer Science, AGH University of Krakow, al. A. Mickiewicza 30, 30-059 Krakow, Poland; asocha@agh.edu.pl (A.M.); kuznia@agh.edu.pl (M.K.)

² Department of Surface Engineering and Analysis of Materials, Faculty of Metals Engineering and Industrial Computer Science, AGH University of Krakow, al. A. Mickiewicza 30, 30-059 Krakow, Poland; debowska@agh.edu.pl

* Correspondence: amagdzia@agh.edu.pl; Tel.: +48-12-617-50-47

Abstract: One of the most popular polymeric materials in the building and construction industry is rigid polyurethane foam (RPUF). In order to reduce the number of expensive chemical components, various fillers are used in the RPUF industry. The aim of this work was to investigate the influence of the biomass originated filler soybean-husk-derived ash on the structure and properties of composite RPUF. Firstly, polyurethane foams were obtained using hand mixing and casting techniques. Composite foams contained 5, 10, 15, and 20 wt. % of the filler. Secondly, the obtained composite materials were analyzed considering their cellular structure using optical microscopy and image processing software. All samples were composed of mostly pentagonal, regular-in-shape cells. Their diameters ranged between 100 and 70 μm . The chemical structure of the foams was investigated using infrared spectroscopy. No chemical interactions between matrix and filler were detected. Mechanical testing was performed in order to evaluate the mechanical performance of the materials. Both compressive strength and Young's modulus were comparable and equaled approx. 130 kPa and 2.5 MPa, respectively. Wettability analysis indicated a hydrophobic nature of the materials. The obtained results suggested that the cellular and chemical structure of the polyurethane matrix was not affected by the filler incorporation.

Keywords: rigid polyurethane foam; biomass ash; composite material



Citation: Magiera, A.; Kuźnia, M.; Błoniarz, A.; Magdziarz, A. Rigid Polyurethane Foams Modified with Soybean-Husk-Derived Ash as Potential Insulating Materials. *Processes* **2023**, *11*, 3416. <https://doi.org/10.3390/pr11123416>

Academic Editor: Yu-Cai He

Received: 28 November 2023

Revised: 11 December 2023

Accepted: 11 December 2023

Published: 13 December 2023



Copyright: © 2023 by the authors. Licensee MDPI, Basel, Switzerland. This article is an open access article distributed under the terms and conditions of the Creative Commons Attribution (CC BY) license (<https://creativecommons.org/licenses/by/4.0/>).

1. Introduction

Polymer technology is now recognized as a rapidly growing field in the construction and building materials industry [1]. It refers to long molecular chains composed of numerous repeating units. Over time, a wide range of polymers including rubber, epoxy resins, SBS block copolymer, SBR, PE, PS, PVC, and EVA have been used worldwide for various civil engineering projects. The use of polymer materials in civil engineering has significantly increased over the years. Among these polymers, polyurethane (PU) has gained considerable interest from engineers and researchers due to its exceptional performance capabilities.

Polyurethane is a type of polymer that contains carbamate groups in its molecular structure [1]. It is typically produced through the reaction between isocyanates and polyols. This organic polymer exhibits outstanding engineering properties such as high corrosion resistance, energy absorption, elongation, chemical resistance, thermal stability, versatility in products and applications, cost-effectiveness, and ease of use. Polyurethanes have a wide variety of uses, such as in elastomers for tires, tubing, cushioning, and patching; foams for insulation, padding, and building purposes; adhesives for bonding glass, ceramics, metals, and wood; coatings for decoration, wear-resistant coatings, and anti-corrosion; sealants for

sealing pavements, buildings, and electronic components; and waterproof materials used to waterproof pavements and other structures.

With the growing concern of environmental sustainability, there has been a shift in focus towards eco-friendly materials in various industries. Materials engineering is one field that has embraced this trend, exploring the use of natural and renewable resources in the development of composites. Polyurethane composites, in particular, have gained attention due to their versatility and wide range of applications. The global production of polyurethane (PU) is the sixth highest in the world in the polymer industry [2]. Various products can be obtained from the PU matrix, such as coatings, adhesives, fibers, foams, and elastomers when adjusting factors such as the reagent ratios, substrate properties, catalyst types, or reaction conditions [3]. Foams make up a significant portion of PU applications at 65% [2]. These foams can be classified into two types: flexible and rigid foam. Flexible foams are soft and easily deformed, commonly used in applications such as furniture cushions and mattresses. On the other hand, rigid foams have high strength, making them suitable for thermal insulation and structural applications.

Rigid polyurethane foam is a versatile thermoset polymer that can be tailored to meet specific requirements. It finds extensive use in thermal insulation, packaging, and transportation due to its low thermal conductivity [4]. Additionally, RPUFs possess favorable properties such as low apparent density and high resistance to chemicals, heat, and mechanical stress, making them suitable for applications in various industries [3,5]. The construction sector utilizes RPUFs for insulation purposes while they are also employed in refrigerator technology and furniture manufacturing [6]. Moreover, automotive companies rely on this material for their products along with space science [7,8]. The versatility of RPUFs extends further into areas such as cooling systems and petrochemicals engineering. In recent years, there has been growing interest in incorporating renewable and sustainable materials in composite technologies to reduce reliance on fossil resources.

Considering the increasing usage of RPUF in recent years, researchers are actively exploring alternative production techniques to lower costs and reduce the reliance on synthetic chemical compounds. Additionally, it is important to note that RPUF's porous nature and large specific surface area make it highly combustible [2,4]. Therefore, improving its fire safety properties has become a crucial area of research to expand its applications and ensure the safety of users.

To expand the excerpt, we can incorporate various fillers into a polymer matrix to create composite RPUF. This approach has been widely studied in the research community, with many papers investigating the effects of filler addition on RPUF properties such as apparent density, thermal and mechanical properties, polyurethane cellular structure, and flammability. For example, Członka et al. successfully incorporated chicken feathers into the RPUF matrix and observed improved mechanical properties in the samples [9]. Another group of researchers developed multi-system composite foams that exhibited excellent flame retardant and self-extinguishing properties [10]. In a different study by Baek et al. [11], silicone–acrylic particles were added to a polyurethane matrix for enhanced sound absorption capabilities of RPUFs. The work conducted by Ribeiro da Silva et al. focused on characterizing polyurethane foams modified with tung oil, ethylene glycol, and rice husk ash through mechanical tests [12]. The impact of coal-originated fly ash on the cellular structure and performance properties (mechanical performance and thermal stability) of RPUF was extensively investigated by Kuźnia et al. [13,14].

In the 1990s, there was a significant increase in globalization, accompanied by economic growth and a corresponding rise in energy demand [15]. As a result, non-renewable energy sources became increasingly depleted over these two decades. Additionally, the cost of generating energy from non-renewable sources continued to escalate, along with its negative environmental impact. To address this global trend towards phasing out fossil fuels in electricity and heat production, the utilization of renewable energy sources has become an unavoidable solution [16,17]. In Poland specifically, biomass plays a crucial role as one of the most important renewable energy sources. In recent years, there has been

substantial progress in utilizing biomass combustion for major power plants. Considering both international and domestic efforts to expand biomass usage for energy production purposes, it is necessary to focus on managing ash generated during this process.

Agricultural activities produce byproducts referred to as agro-waste, which comprises residual straws, shells, stalks, manures, leaves, seeds, and other significant sources [18]. It has been reported that approximately two billion tons of agro-waste is generated globally each year and contains varying quantities of cellulose, hemicellulose, lignin, and extractives. Agro-waste is categorized into two groups based on its origin: agro-residues from agriculture fields and industrial residues from industries after raw material processing. Agro-residues can be categorized as either field residues, which are remnants left on fields post crop harvesting such as husks, stalks, leaves, and stems; or process residues, the leftovers of field residue after crops are converted to their final form. Industrial residues constitute waste generated during industrial or manufacturing activities such as those for potato peels, soybean oil cake, tea processing waste, and coconut oil cake.

The management of agro-waste involves a variety of methods, such as incineration, haphazard disposal, and utilization as animal feed [18]. However, these waste management practices have various adverse effects: burning agricultural waste results in the release of pollutants and greenhouse gases, while also depleting soil nutrients and microbial populations due to aerosol formation. Similarly, unregulated dumping leads to decomposition and environmental problems. Inadequate waste control can contribute to the pollution of water, air, and soil ecosystems, which further exacerbates climate change impacts. Conversely, using agro-waste provides dual advantages by offering cost-effective biodegradable materials that create employment opportunities while mitigating negative consequences such as stubble burning, emissions of greenhouse gases, and pollutant generation if left untreated.

The researchers have demonstrated that only 8.6% of the global economy was circular by 2020, indicating that a small portion of waste was being cycled [18]. The circular economy model aims to minimize waste and offer a sustainable alternative through sharing, renovating, repairing, reusing, and recycling existing products as much as possible. Efforts are ongoing to utilize agro-waste for creating value-added products; however, this practice is currently limited to the lab-scale or to small businesses and has potential for further exploration into new applications that directly benefit farmers while promoting a circular economy paradigm.

In the field of materials engineering, there is a growing interest in utilizing biomass resources for the development of eco-friendly materials. These materials, often referred to as “green” composites, utilize natural fillers and reinforcing elements combined with biopolymer matrices from renewable sources. These green composites offer numerous advantages, such as being economical, environmentally friendly, biodegradable, and readily available. One approach to managing biomass ash is by incorporating it into composite materials. This approach not only allows for the efficient utilization of biomass residues but also contributes to the development of more sustainable and environmentally friendly composite materials. Previous studies have primarily concentrated on integrating raw biomass into composite polyurethane materials. Different fillers, such as ground hazelnut, cellulose, chitin, eggshell [19], and a combination of sawdust from fir, oak, and beech wood were utilized [20]. Additionally, other natural fibers including coir fiber [21], jute, hemp, sisal, flax, bamboo, cotton [22], kenaf, ramie, abaca, or henequen [23] have been explored for their potential application in these materials.

In addition to the aforementioned approaches, biomass-derived polyols (known as biopolyols) have been utilized in the preparation of polyurethane foam [24,25]. The work by Cabrera [26] highlights that food and wood industry residues serve as abundant sources for biopolyol precursors on a large scale. Jasiunas et al. explored hemp stalk hurds and sugar beet pulp as potential originators for biopolyols [27,28]. Zhang et al., on the other hand, obtained polyols from crop straws such as oilseed rape straw, rice straw, wheat straw, and corn stover [29]. Olszewski et al. utilized mixed wood shavings in their research efforts [30] while exploring biomass-generated ash as a modifying agent. This remains

relatively unexplored, with only Kairyte et al.'s study using waste ash from the wood industry's grate and primary combustion chambers being reported so far [31,32]. Hejna et al. [33,34] also incorporated wood ash produced through gasification processes utilizing pellets. Presently, in polyurethane technology, the utilization of soybean husk has only been limited to that of a biopolyol precursor [35].

In the manufacturing of animal feed, soy is one of the major sources of vegetable protein, and its role in human nutrition is systematically growing as well [36]. Soy crops are grown globally. According to estimates, 362 million metric tons of soy were harvested worldwide in 2018–2019, accounting for over 60% of all oleaginous seed output. The main components of soybean seeds are proteins, lipids, carbohydrates, and ashes, which make up an average of 40%, 20%, 15%, and 5% respectively, comprising the dry mass. Approximately 85% of the global soy production designated for crushing results in creating soybean meal (Figure 1). The majority (~98%) is used for making animal feed while around 2% is utilized by facilities producing soybean protein.

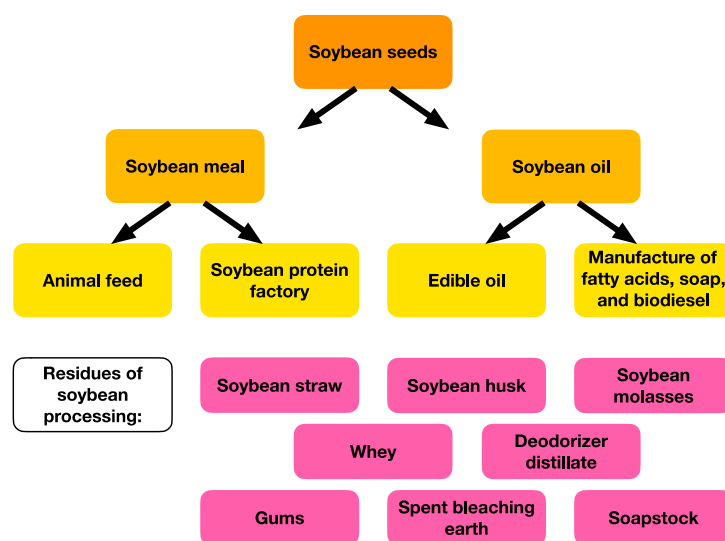


Figure 1. Schematic depiction of soybean processing chain.

Soybean straw refers to the initial residue of soybean processing, resulting from the removal of stems, leaves, and husks. After degumming, the generated gums are typically used in lecithin production. Meanwhile, soapstock is a residue produced during the neutralization of crude or degummed soybean oil. Spent bleaching earth results from the refining process aimed at adjusting oil color by removing carotenoids and chlorophyll; this residue contains sterols, tocopherols, and triglycerols and is commonly discarded in landfills. Deodorization helps remove aldehydes, ketones, and other volatile substances that can affect the sensory properties of soybean oil—these form deodorizer distillate as a byproduct. Additionally, the protein concentration process yields a thick brown syrup known as soybean molasses, while extracting HCl generates a liquid part called soy whey.

Soybean husk, a byproduct of the soy processing chain, offers various potential applications. It can be utilized as a source for enzymes, pectin, oligopeptides, ethanol, butanediol, and polymalic acid [36]. In addition to these uses, biomass ashes derived from soybean husks have been proposed as an alternative to cement in cement-based composites [37]. This is due to the high silica content and large surface area of the ash particles. Moreover, soybean husks have also been explored as sources for cellulose nanocrystals (CNC) and cellulose nanofibrils (CNF) [38]. In summary, the use of biomass materials such as hemp stalk hurds, sugar beet pulp, crop straws, wood shavings, and soybean husks in various applications and composite technologies is an area of ongoing research and exploration.

The use of soybean-based composites not only reduces reliance on non-renewable resources but also offers several environmental benefits. One of these benefits is the reduction in carbon emissions. By replacing petroleum-based plastics with soybean-based

composites, the carbon footprint of materials engineering is significantly reduced. Furthermore, soybean-based composites are also recyclable and biodegradable, minimizing waste and contributing to a more sustainable materials cycle.

The objective of this study was to explore the potential use of soybean-husk-derived ash as a modifier in RPUF (rigid polyurethane foam) technology. The previous literature has primarily focused on using the soybean husk as a biopolyol precursor in PUR technology [35], with limited information available on its application in RPUF technology. The filler used in this research was laboratory-obtained bottom ash from the incineration process. Composite materials containing up to 20% wt. of the modifier were prepared and analyzed for their cellular structure, chemical composition, mechanical performance, and wettability parameters.

2. Materials and Methods

We prepared rigid polyurethane foams using the two-component commercial system EKOPRODUR PM4032 with a mixing and casting technique. In this research, we used soybean husk bottom ash as a modifier for the polyurethane foam. The ash was generated in laboratory conditions according to the EN ISO 18122:2016 standard [39]. To prepare composite RPUF, we stirred appropriate amounts of the ash (5, 10, 15, and 20% wt.) into the polyol components using a laboratory stirrer for one minute at a speed of 4500 rpm. Next, we mixed both the polyol and isocyanate components (weight ratio of 100:110) using a laboratory stirrer for one minute at a speed of 4500 rpm before casting them into rectangular molds measuring 20 cm × 20 cm × 5 cm. The molds were then left under a fume hood. After waiting for 48 hours, we removed the foams from the molds and let them sit under a fume hood for an additional five days to eliminate any unreacted isocyanate component. The resulting composite foams were labeled as PUR + 5%A, PUR + 10%A, and PUR + 15%A. The composite production process is depicted in Figure 2.

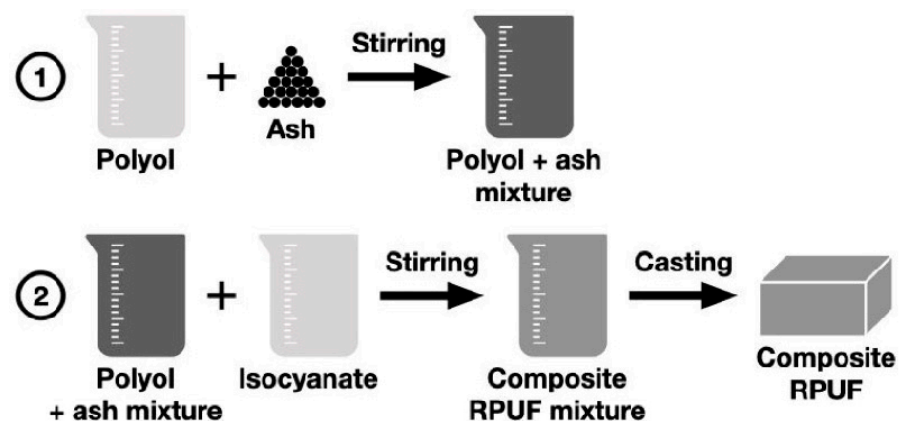


Figure 2. Schematic depiction of the composites production process: stage ①—mixing of the filler with polyol; stage ②—preparation of the composite RPUF.

Samples of the RPUF with a stabilized structure were cropped and subjected to analysis. The cellular structure of the specimens was characterized using optical microphotographs taken with the Keyence VHX-900F microscope on 5-mm-thick slices. Analysis of the microphotographs was carried out using free software called ImageJ (version 1.48v). From 30 measurements, average values \pm standard deviation were calculated for strut thickness as well as horizontal and vertical Feret diameters to characterize the RPUF cellular structure.

Scanning electron microscopy (SEM; FEI Inspect S50, Thermo Fisher Scientific Inc., Waltham, MA, USA) was used to observe the microstructure of the produced foams. During image acquisition, SE mode with a voltage range of 2–5 kV and spot size set at 3.0 were utilized. Before measurement, gold sputtering was applied to the samples to ensure improved image quality.

Fourier-transform infrared spectra were obtained using a Tensor 27 spectrometer, equipped with OPUS 7.2 software. The spectra were collected in the absorbance mode within the range of 4000–400 cm^{-1} after averaging 64 scans at a resolution of 4 cm^{-1} . The KBr pellet method was utilized for sample preparation. The analyzed materials included unmodified RPUF foam, soybean-husk-derived bottom ash referred to as A, and composite foam PUR + 20% A (other composites were not evaluated due to low filler content). These registered spectra were then scrutinized to determine the chemical structure of the composite RPUF material.

Apparent densities of the composites were determined using the ASTM D1622-03 standard [40]. The samples of polymeric foams were weighed and measured for their dimensions. The average of 5 tests and the corresponding standard deviation value were reported as the results of the measurements.

Mechanical tests of the composite RPUF were performed on a universal testing machine, specifically the Zwick 1435 model from Zwick Roell in Germany. The load cell used had a capacity of 5 kN. To test the foams, samples in the form of rollers with diameters measuring 30 mm and heights measuring 12 mm were subjected to compression at a speed of 2 mm/min until reaching a deformation level of 75%. From these stress–strain curves obtained, compressive strength and Young's modulus (E) values were calculated. The results reported here are based on an average from five tests along with their standard deviation.

A Kruss DSA 25 goniometer was used to perform the contact angle (CA) and for the surface free energy (SFE) determination. Contact angles in water, as a polar liquid and in diiodomethane, as a non-polar liquid were measured. For the investigation of surface free energy, SFE, the Owens–Wendt–Rabel–Kaelble (OWRK) method was applied.

To determine the chemical composition of soybean-husk-derived ash (labeled A), we utilized the X-ray fluorescence technique. Our measurements were conducted on a WD-XRF ZSX Primus II spectrometer equipped with an Rh lamp from Rigaku, Japan. The semi-quantitative analysis was performed using SQX software Pro Version within the F-U range, allowing us to normalize the concentrations of all identified elements up to 100%.

The X-ray diffraction technique was used to identify the crystalline phases present in the biomass-generated ash. The analysis was performed on a PANanalytical EMPYREAN DY 1061 (Anton Paar, Graz, Austria) diffractometer equipped with a Cu lamp emitting $K\alpha$ line (40 kV, 40 mA, $\lambda = 0.154$ nm) in Bragg–Brentano geometry. An angular range of $2\theta = 10\text{--}90^\circ$ was applied, with a count time of $t = 10$ s and a step width of 0.07° for each measurement.

3. Results

3.1. Cellular Structure

A sample optical microphotograph of the composite RPUF (PUR + 5%A) is shown in Figure 3. The obtained materials consisted of a cellular structure, which is characteristic of polyurethane foams. The cells were mostly pentagonal and exhibited regular morphology. Details on the cellular morphology parameters can be found in Table 1. Both vertical and horizontal Feret diameters were relatively similar, indicating no dominant growth direction. With an increase in ash content from 5 to 20%, there was a decrease observed in vertical Feret diameters with values ranging between 71–95 μm , while horizontal Feret diameters ranged between 63–98 μm respectively. The cell size remained uniform across different filler concentrations, with most cells falling within the range of approximately 50–100 μm as illustrated by Figure 4. The thickness of the cell struts was not influenced by filler content and stayed consistent at around 11–12 μm . The dispersal pattern for fillers showed an even distribution throughout the polymer matrix.

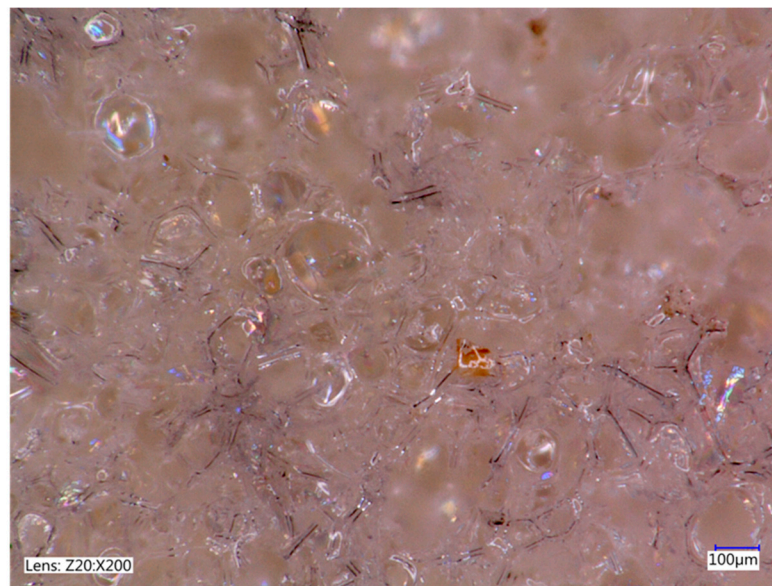


Figure 3. Optical microphotograph of composite RPUF, PUR + 5%A (magnitude $\times 200$).

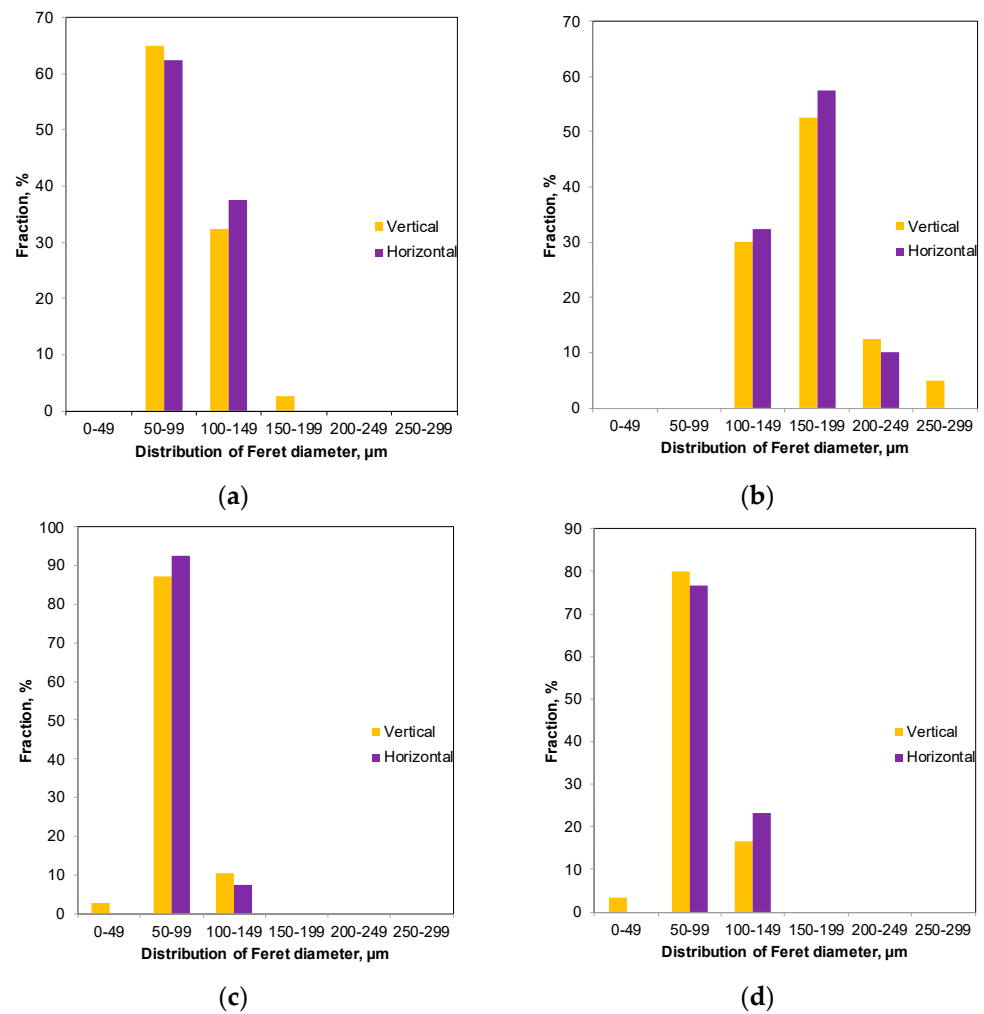
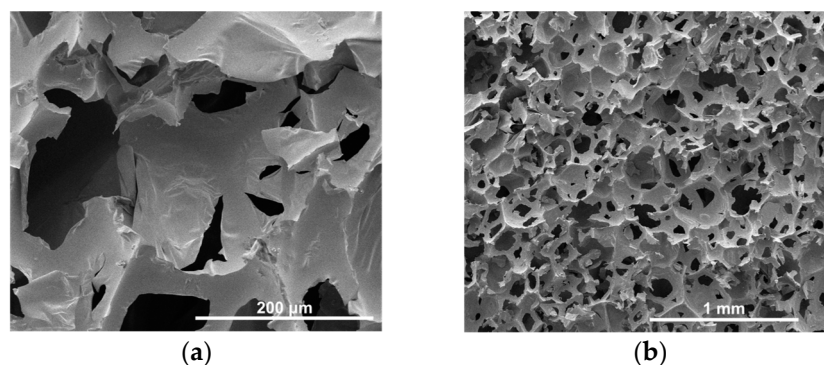


Figure 4. Feret diameters' histograms of (a) PUR + 5%A, (b) PUR + 10%A, (c) PUR + 15%A, and (d) PUR + 20%A.

Table 1. Foams' cellular morphology parameters.

Sample Name	Vertical Feret Diameter, μm	Horizontal Feret Diameter, μm	Strut Thickness, μm
PUR + 5%A	95 ± 5	98 ± 4	10.5 ± 0.6
PUR + 10%A	71 ± 11	63 ± 9	12.9 ± 0.5
PUR + 15%A	77 ± 5	75 ± 4	11.2 ± 0.5
PUR + 20%A	79 ± 6	85 ± 6	10.7 ± 0.4

Sample SEM microphotographs of composite RPUF (PUR + 5%A) are presented in the Figure 5. The cellular structure of the polymer matrix was successfully formulated in composite foams. Polymeric matrixes were uniform with evenly distributed filler particles; no aggregates of the latter were observed. Due to the preparation of the samples examined on SEM (covered with gold to ensure better imaging), the test results were not used to calculate cellular parameters. These parameters were determined based on the results from the optical microscope. They supported observations and conclusions formulated based on optical microscope observations. The presence of biomass-generated ash in composite RPUF materials did not significantly affect the cellular structure or morphology.

**Figure 5.** SEM microphotographs of composite RPUF, PUR + 5%A. Magnitudes (a) $\times 300$, and (b) $\times 50$.

3.2. Chemical Structure

The FTIR spectrum of the composite PUR + 20%A foam is shown in Figure 6. The absorption bands observed in the spectrum can be attributed to various components of the polyurethane matrix. These include stretching vibrations of N–H groups at 3350 cm^{-1} , symmetric and asymmetric stretching vibrations of C–H bonds in aliphatic chains at $3000\text{--}2800\text{ cm}^{-1}$, vibrations related to the phenyl ring in the isocyanate structure at 2300 , 2150 , and 1600 cm^{-1} , stretching vibration of C=O bonds at 1700 cm^{-1} , bending vibration of N–H groups at 1500 cm^{-1} , vibrations associated with CH₂ and CH₃ groups at 1400 cm^{-1} , stretching vibration of C–N bonds at 1300 cm^{-1} , stretching vibration of C–O bonds at 1200 cm^{-1} , vibrations related to ether bonds in the polyol structure at $1100\text{--}1000\text{ cm}^{-1}$, and vibrations associated with C–C bonds and aromatic rings in the isocyanate structure at $900\text{--}700\text{ cm}^{-1}$ [18,33,34,41,42].

Based on XRF analysis, soybean-husk-derived ash was composed mainly of CaO, K₂O, P₂O₅, MgO, SO₃, and SiO₂ (Table 2). These results correspond with crystal phases identified using the XRD technique and listed in Table 2 and Figure 7. They were mainly fairchildite, calcite, arcanite, potassium calcium phosphate, and potassium carbonate. Absorption bands, registered using FTIR spectroscopy (Figure 6; spectrum labeled as “Ash”), were characteristic for the biomass-derived ash structure [43–47]. A wide, low intensity band at $3600\text{--}3000\text{ cm}^{-1}$ was associated with OH groups present within the ash structure. Asymmetric stretching vibrations of carbonate compounds were present at $1500\text{--}1300\text{ cm}^{-1}$. In the silica bonds Si–O asymmetric stretching vibrations occurred at $1200\text{--}900\text{ cm}^{-1}$. An absorption band at 850 cm^{-1} was related to asymmetric stretching and

bending vibrations of carbonate groups. Silica formations were evidenced by absorption peaks at 700, 600–500, and 500–400 cm^{-1} .

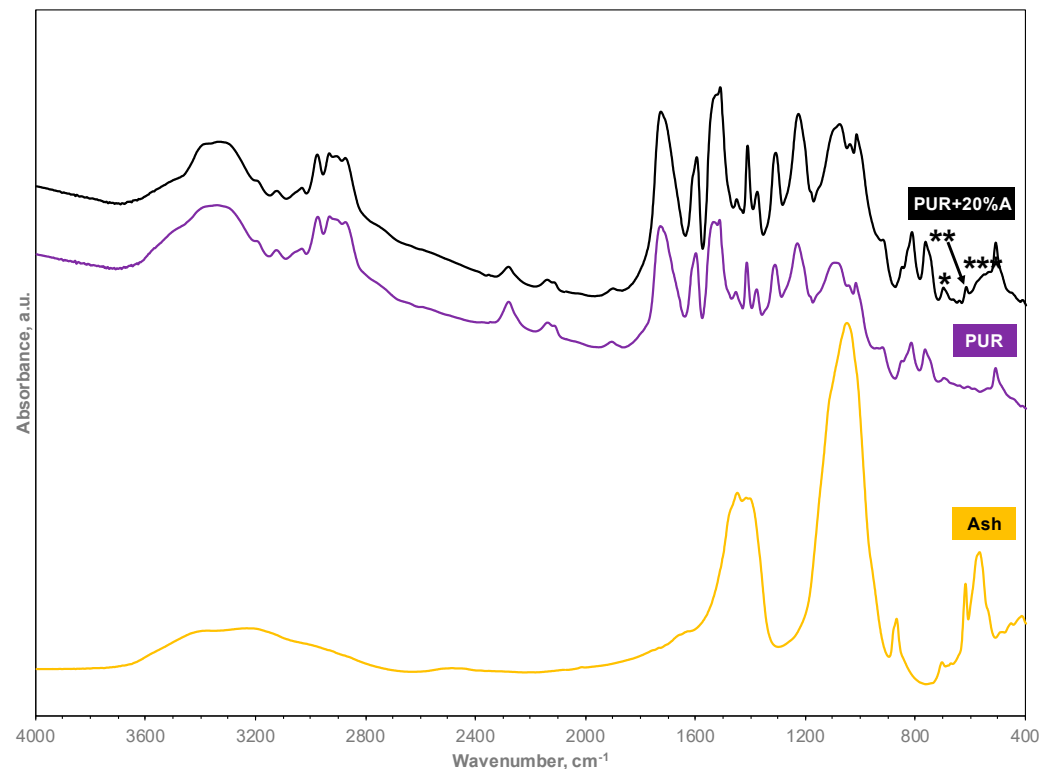


Figure 6. FTIR spectra of soybean-husk-derived ash (labeled Ash), unmodified RPUF (labeled PUR), and RPUF modified with 20% wt. of soybean-husk-derived ash (labeled PUR + 20%A). Additional bands in the spectrum of the PUR + 20%A at about 700 (*), 600 (**), and 600–500 cm^{-1} (***) were related to silica.

Table 2. Oxide analysis (XRF) and crystal phases (XRD) composition of soybean-husk-derived ash.

Oxide Composition	Fraction, %	Crystal Phases
CaO	39.2	Fairchildite $\text{K}_2\text{Ca}(\text{CO}_3)_2$
K_2O	34.2	Calcite CaCO_3
P_2O_5	17.1	Arcanite K_2SO_4
MgO	5.6	Potassium calcium phosphate KCaPO_4
SO_3	1.5	Potassium carbonate K_2CO_3
SiO_2	1.1	Larnite Ca_2SiO_4
Fe_2O_3	0.5	Brianite $\text{Na}_2\text{CaMg}(\text{PO}_4)_2$
Al_2O_3	0.4	Syngenite $\text{K}_2\text{Ca}(\text{SO}_4)_2 \cdot \text{H}_2\text{O}$
Na_2O	0.1	Potassium hydrogen monosilicate KHSiO_3
MnO	0.1	

The FTIR spectrum of the PUR + 20%A composite foam (Figure 6; top) largely resembles the unmodified PUR foam due to the high polymer content in the composite (80% wt.). The slight changes in the spectrum, such as additional bands at about 700 (*), 600 (**), and 600–500 cm^{-1} (***), indicate the presence of filler in the polymer matrix. These new bands are attributed to the ash molecular structure, specifically silica. No additional bands unrelated to ash structure were observed, suggesting that there was no chemical bonding between the polymer and filler.

3.3. Mechanical Properties and Wettability Analysis

The mechanical performance properties of composite RPUF were characterized through mechanical testing to investigate the influence of ash on these parameters. The incorpo-

ration of the filler affected the compressive strength of the material, although the trend of this change was not definitive (Table 3). As the ash content increased from 5% to 20%, the compressive strength values for R_m were recorded as 148 kPa, 135 kPa, 127 kPa, and a slight increase to 142 kPa. The standard deviation values ranged between 9% and 30%, indicating comparable calculated R_m values. Likewise, E was also influenced by increasing levels of content, ranging from 1.9 MPa at 5% ash content to 2.4 MPa at 10% ash content, and further increasing to 2.5 MPa at 15%, finally rising once again to 2.9 MPa at 20%. The SD values for E fell within the range of 9–25%.

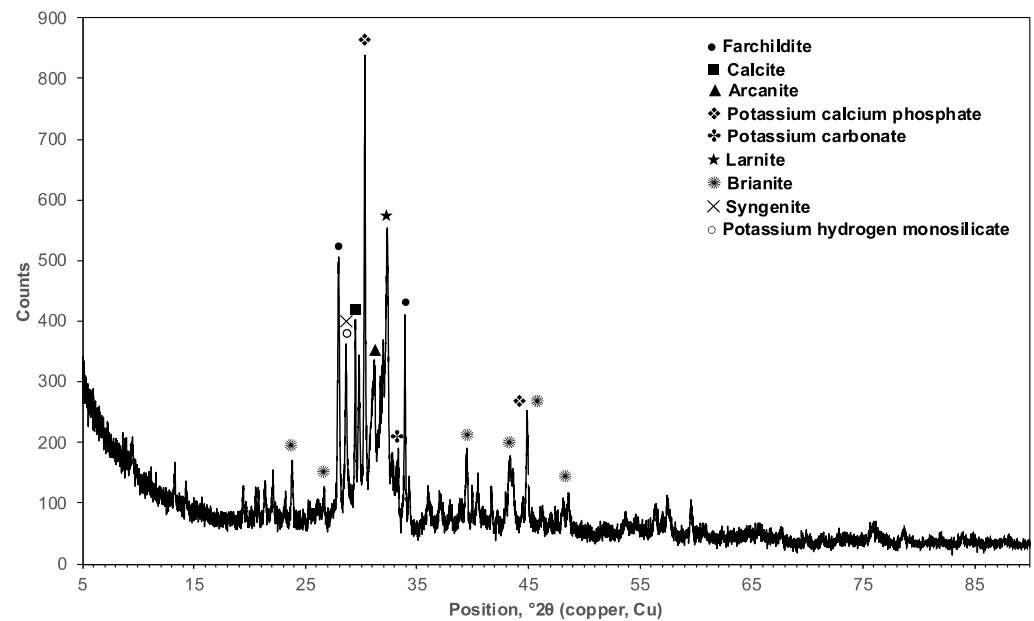


Figure 7. XRD diffractogram of soybean-husk-derived ash.

Table 3. Foams' densities and mechanical performance parameters.

Sample Name	Apparent Density d , kg m^{-3}	Compressive Strength R_m , kPa	Young's Modulus E , MPa
PUR + 5%A	41 ± 1	148 ± 19	1.9 ± 0.5
PUR + 10%A	37 ± 1	135 ± 13	2.4 ± 0.3
PUR + 15%A	46 ± 2	128 ± 27	2.5 ± 0.6
PUR + 20%A	55 ± 5	142 ± 43	2.9 ± 0.4

The wettability parameters, calculated in this research, are presented in Table 4. Water contact angles varied between 100–150° and increased with the addition of biomass ash. Diiodomethane contact angles were also affected by the presence of biomass ash and ranged around 90°. Surface free energy values were similar for composite foams containing 10–20% of the filler. Microscopic observations showed disruption in the cellular structure for PUR + 5%A foam, which was consistent with the deviating wettability parameters.

Table 4. Foams' wettability parameters.

Sample Name	Contact Angle in H_2O , °	Contact Angle in $\text{C}_2\text{H}_2\text{I}_2$, °	SFE Total, mN m^{-1}	SFE Disperse, mN m^{-1}	SFE Polar, mN m^{-1}
PUR + 5%A	106.3 ± 1.9	64.1 ± 7.4	26.3 ± 4.5	26.2 ± 4.3	0.1 ± 0.2
PUR + 10%A	119.3 ± 4.4	93.6 ± 1.1	11.3 ± 0.7	11.2 ± 0.5	0.2 ± 0.3
PUR + 15%A	131.6 ± 1.4	88.0 ± 4.4	14.1 ± 2.3	13.6 ± 2.0	0.5 ± 0.3
PUR + 20%A	151.2 ± 5.2	92.1 ± 5.6	14.4 ± 3.4	11.8 ± 2.4	2.6 ± 1.0

4. Discussion

This study aimed to investigate the impact of incorporating soybean-husk-derived bottom ash on the structure and properties of RPUF. The presence of ash did not affect the cellular structure, which is defined by the polyurethane matrix. However, as the filler content increased, there was a decrease in cell size indicating that ash particles acted as nucleation sites during polyurethane cell formation [48–50]. Interestingly, larger diameters were calculated for PUR + 5%A samples suggesting disruption of the cellular structure and hindered cell formation. This could be attributed to weak binding forces between ash particles and the polyurethane matrix, resulting in the collapse of the cellular structure.

Chemical structure analysis did not show any chemical interactions between the filler and polyurethane matrix. Since absorption bands related to the ash overlapped with polyurethane-originated bands, they were not visible in the composite spectrum. What is more, due to the relatively small amount of the filler added to the polymer matrix, the intensities of the ash-originated bands were low and led to a background shift. These results suggest that the addition of soybean-husk-derived bottom ash to RPUF does not significantly impact the chemical structure of the composite material.

The mechanical characteristics of the RPUF were found to be unaffected by the amount of ash. The compressive strength of unmodified RPUF was approximately 190 kPa, and Young's modulus was around 2.4 MPa. The addition of filler only had a slight impact on these parameters, indicating limited interfacial interactions and bonding. These mechanical performance parameters align with values reported by other researchers for PUR composite foams [51–55]. It was observed that incorporating the filler increased the composite Young's modulus, while the amount of ash did not affect this mechanical characteristic. Moreover, as the filler content increased, there was also an increase in apparent density due to loading polymeric systems with ash particles.

Polyurethanes, being hydrophobic materials, have water contact angles exceeding 90° [56–60], which is important for their use in the construction industry. The analysis of wettability showed that all composite foams had a strong hydrophobic nature. Water contact angle values increased with the amount of biomass-derived filler added. This indicates that incorporating soybean-husk-derived bottom ash into RPUF improves its hydrophobic characteristics and makes it suitable for applications in environments with high moisture levels such as in construction and building materials.

5. Conclusions

In conclusion, the addition of soybean-husk-derived bottom ash to RPUF composites does not significantly alter the chemical structure of the material. Furthermore, the mechanical properties of the RPUF, such as compressive strength and Young's modulus, are minimally affected by the addition of ash filler. However, the incorporation of ash does lead to an increase in the apparent density of the composite. RPUF containing soybean-husk-derived ash is a promising composite material. To fully investigate its potential, further research including flammability and thermal stability tests should be performed.

Author Contributions: Conceptualization, A.M. (Anna Magiera) and M.K.; methodology, A.M. (Anna Magiera); validation, A.M. (Anna Magiera) and M.K.; investigation, A.M. (Anna Magiera), A.B. and A.M. (Aneta Magdziarz); resources, A.M. (Anna Magiera), M.K., A.B. and A.M. (Aneta Magdziarz); writing—original draft preparation, A.M. (Anna Magiera); writing—review and editing, A.M. (Anna Magiera), M.K. and A.M. (Aneta Magdziarz); visualization, A.M. (Anna Magiera); supervision, A.M. (Aneta Magdziarz); project administration, A.M. (Anna Magiera); funding acquisition, A.M. (Aneta Magdziarz). All authors have read and agreed to the published version of the manuscript.

Funding: This research was funded by the Ministry of Science and Higher Education, Poland (AGH grant no. 16.16.110.663).

Data Availability Statement: The data presented in this study are available on request from the corresponding author. The data are not publicly available due to privacy.

Acknowledgments: We would like to thank Wojciech Jerzak (AGH University of Krakow, Faculty of Metals Engineering and Industrial Computer Science, Department of Heat Engineering and Environment Protection) for his help in performing XRF investigation.

Conflicts of Interest: The authors declare no conflict of interest.

References

1. Li, X.; Li, J.; Wang, J.; Yuan, J.; Jiang, F.; Yu, X.; Xiao, F. Recent applications and developments of Polyurethane materials in pavement engineering. *Constr. Build. Mater.* **2021**, *304*, 124639. [[CrossRef](#)]
2. Wang, S.; Yang, X.; Li, Z.; Xu, X.; Liu, H.; Wang, D.; Min, H.; Shang, S. Novel eco-friendly maleopimaric acid based polysiloxane flame retardant and application in rigid polyurethane foam. *Compos. Sci. Technol.* **2020**, *198*, 108272. [[CrossRef](#)]
3. Pagacz, J.; Hebda, E.; Michałowski, S.; Ozimek, J.; Sternik, D.; Pielichowski, K. Polyurethane foams chemically reinforced with POSS—Thermal degradation studies. *Thermochim. Acta* **2016**, *642*, 95–104. [[CrossRef](#)]
4. Zhou, Y.; Bu, R.; Yi, L.; Sun, J. Heat transfer mechanism of concurrent flame spread over rigid polyurethane foam: Effect of ambient pressure and inclined angle. *Int. J. Therm. Sci.* **2020**, *155*, 106403. [[CrossRef](#)]
5. Stanzione, M.; Russo, V.; Oliviero, M.; Verdolotti, L.; Sorrentino, A.; di Serio, M.; Tesser, R.; Iannace, S.; Lavorgna, M. Synthesis and characterization of sustainable polyurethane foams based on polyhydroxyls with different terminal groups. *Polymer* **2018**, *149*, 134–145. [[CrossRef](#)]
6. Członka, S.; Strąkowska, A.; Strzelec, K.; Kairyte, A.; Vaitkus, S. Composites of rigid polyurethane foams and silica powder filler enhanced with ionic liquid. *Polym. Test.* **2019**, *75*, 12–25. [[CrossRef](#)]
7. Zhang, L.; Zhang, M.; Zhou, Y.; Hu, L. The study of mechanical behavior and flame retardancy of castor oil phosphate-based rigid polyurethane foam composites containing expanded graphite and triethyl phosphate. *Polym. Degrad. Stab.* **2013**, *98*, 2784–2794. [[CrossRef](#)]
8. Zatorski, W.; Brzozowski, Z.K.; Kolbrecki, A. New developments in chemical modification of fire-safe rigid polyurethane foams. *Polym. Degrad. Stab.* **2008**, *93*, 2071–2076. [[CrossRef](#)]
9. Członka, S.; Sienkiewicz, N.; Strąkowska, A.; Strzelec, K. Keratin feathers as a filler for rigid polyurethane foams on the basis of soybean oil polyol. *Polym. Test.* **2018**, *72*, 32–45. [[CrossRef](#)]
10. Qian, L.; Li, L.; Chen, Y.; Xu, B.; Qiu, Y. Quickly self-extinguishing flame retardant behavior of rigid polyurethane foams linked with phosphaphenanthrene groups. *Compos. Part B* **2019**, *175*, 107186. [[CrossRef](#)]
11. Baek, S.H.; Kim, J.H. Polyurethane composite foams including silicone-acrylic particles for enhanced sound absorption via increased damping and frictions of sound waves. *Compos. Sci. Technol.* **2020**, *198*, 108325. [[CrossRef](#)]
12. Da Silva, V.R.; Mosiewicki, M.A.; Yoshida, M.I.; da Silva, M.C.; Stefani, P.M.; Marcovich, N.E. Polyurethane foams based on modified tung oil and reinforced with rice husk ash II: Mechanical characterization. *Polym. Test.* **2013**, *32*, 665–672. [[CrossRef](#)]
13. Kuźnia, M.; Magiera, A.; Pielichowski, K.; Ziabka, M.; Benko, A.; Szatkowski, P.; Jerzak, W. Fluidized bed combustion fly ash as filler in composite polyurethane materials. *Waste Manag.* **2019**, *92*, 115–123. [[CrossRef](#)]
14. Kuźnia, M.; Magiera, A.; Zygmunt-Kowalska, B.; Kaczorek-Chrobak, K.; Pielichowska, K.; Szatkowski, P.; Benko, A.; Ziabka, M.; Jerzak, W. Fly ash as an eco-friendly filler for rigid polyurethane foams modification. *Materials* **2021**, *14*, 6604. [[CrossRef](#)] [[PubMed](#)]
15. Igliński, B.; Pietrzak, M.B.; Kielkowska, U.; Skrzatek, M.; Kumar, G.; Piechota, G. The assessment of renewable energy in Poland on the background of the world renewable energy sector. *Energy* **2022**, *261*, 125319. [[CrossRef](#)]
16. Jankowski, K.J.; Sokolski, M.; Szatkowski, A.; Kozak, M. Crambe—Energy efficiency of biomass production and mineral fertilization. A case study in Poland. *Ind. Crops Prod.* **2022**, *182*, 114918. [[CrossRef](#)]
17. Dzikuć, M.; Gorączkowska, J.; Piwowar, A.; Dzikuć, M.; Smoleński, R.; Kułyk, P. The analysis of the innovative potential of the energy sector and low-carbon development: A case study for Poland. *Energy Strategy Rev.* **2021**, *38*, 100769. [[CrossRef](#)]
18. Asefnejad, A.; Khorasani, M.T.; Behnamghader, A.; Farsadzadeh, B.; Bonakdar, S. Manufacturing of biodegradable polyurethane scaffolds based on polycaprolactone using a phase separation method: Physical properties and in vitro assay. *Int. J. Nanomed.* **2011**, *6*, 2375. [[CrossRef](#)]
19. Husainie, S.M.; Deng, X.; Ghalia, M.A.; Robinson, J.; Naguib, H.E. Natural fillers as reinforcement for closed-molded polyurethane foam plaques: Mechanical, morphological, and thermal properties. *Mater. Today Commun.* **2021**, *27*, 102187. [[CrossRef](#)]
20. Stancin, H.; Mikulčić, H.; Manić, N.; Stojiljković, D.; Vujanović, M.; Wang, X.; Duić, N. Thermogravimetric and kinetic analysis of biomass and polyurethane foam mixtures co-pyrolysis. *Energy* **2021**, *237*, 121592. [[CrossRef](#)]
21. Pereira, R.C.; Felipe, V.T.A.; Avelino, F.; Mattos, A.L.; Mazzetto, S.E.; Lomonaco, D. From biomass to eco-friendly composites: Polyurethanes based on cashew nutshell liquid reinforced with coconut husk fiber. *Biomass Convers. Biorefin.* **2022**. [[CrossRef](#)]
22. Ramachandran, A.; Mavinkere Rangappa, S.; Kushvaha, V.; Khan, A.; Seingchin, S.; Dhakal, H.N. Modification of fibers and matrices in natural fiber reinforced polymer composites: A comprehensive review. *Macromol. Rapid Commun.* **2022**, *43*, 2100862. [[CrossRef](#)]
23. Asim, M.; Paridah, M.T.; Chandrasekar, M.; Shahroze, R.M.; Jawaid, M.; Nasir, M.; Siakeng, R. Thermal stability of natural fibers and their polymer composites. *Iran. Polym. J.* **2020**, *29*, 625–648. [[CrossRef](#)]

24. Malani, R.S.; Malshe, V.C.; Thorat, B.N. Polyols and polyurethanes from renewable sources: Past, present, and future—Part 2: Plant-derived materials. *J. Coat. Technol. Res.* **2022**, *19*, 361–375. [[CrossRef](#)]
25. Malani, R.S.; Malshe, V.C.; Thorat, B.N. Polyols and polyurethanes from renewable sources: Past, present and future—Part 1: Vegetable oils and lignocellulosic biomass. *J. Coat. Technol. Res.* **2022**, *19*, 201–222. [[CrossRef](#)]
26. Cabrera, F.C. Eco-friendly polymer composites: A review of suitable methods for waste management. *Polym. Compos.* **2021**, *42*, 2653–2677. [[CrossRef](#)]
27. Jasiunas, L.; Peck, G.; Bridziuvienė, D.; Miknius, L. Mechanical, thermal properties and stability of high renewable content liquefied residual biomass derived bio-polyurethane wood adhesives. *Int. J. Adhes. Adhes.* **2020**, *101*, 102618. [[CrossRef](#)]
28. Jasiunas, L.; McKenna, S.T.; Bridziuvienė, D.; Miknius, L. Mechanical, thermal properties and stability of rigid polyurethane foams produced with crude-glycerol derived biomass biopolyols. *J. Polym. Environ.* **2020**, *28*, 1378–1389. [[CrossRef](#)]
29. Zhang, J.; Hori, N.; Takemura, A. Effect of natural biomass fillers on the stability, degradability, and elasticity of crop straws liquefied polyols-based polyurethane foams. *J. Appl. Polym. Sci.* **2023**, *140*, e53324. [[CrossRef](#)]
30. Olszewski, A.; Kosmela, P.; Piszczczyk, Ł. Synthesis and characterization of bio-polyols through biomass liquefaction of wood shavings and their application in the preparation of polyurethane wood composites. *Eur. J. Wood Wood Prod.* **2021**, *80*, 57–74. [[CrossRef](#)]
31. Kairyte, A.; Kremensas, A.; Vaitkus, S.; Członka, S.; Strąkowska, A. Fire suppression and thermal behavior of biobased rigid polyurethane foam filled with biomass incineration waste ash. *Polymers* **2020**, *12*, 683. [[CrossRef](#)]
32. Kairyte, A.; Kizinievic, O.; Kizinievic, V.; Kremensas, A. Synthesis of biomass-derived bottom waste ash based rigid biopolyurethane composite foams: Rheological behaviour, structure and performance characteristics. *Compos. Part A* **2019**, *117*, 193–201. [[CrossRef](#)]
33. Hejna, A.; Kopczyńska, M.; Kozłowska, U.; Klein, M.; Kosmela, P.; Piszczczyk, Ł. Foamed polyurethane composites with different types of ash—morphological, mechanical and thermal behavior assessments. *Cell. Polym.* **2016**, *35*, 287–308. [[CrossRef](#)]
34. Hejna, A.; Kosmela, P.; Mikicka, M.; Danowska, M.; Piszczczyk, Ł. Modification of microporous polyurethane elastomers with different types of ash—Morphological, mechanical, and thermal studies. *Polym. Compos.* **2016**, *37*, 881–889. [[CrossRef](#)]
35. Chi, J.; Zhang, Y.; Tu, F.; Sun, J.; Zhi, H.; Yang, J. The synergistic flame-retardant behaviors of soybean oil phosphate-based polyols and modified ammonium polyphosphate in polyurethane foam. *J. Polym. Res.* **2023**, *30*, 84. [[CrossRef](#)]
36. Biazatti, M.J.; de Carvalho Miranda, J.C. Soybean-based concept biorefinery. *Biofuels, Bioprod. Biorefin.* **2021**, *15*, 980–1005. [[CrossRef](#)]
37. Supić, S.; Malesev, M.; Radonjanin, V.; Bulatović, V.; Milović, T. Reactivity and pozzolanic properties of biomass ashes generated by wheat and soybean straw combustion. *Materials* **2021**, *14*, 1004. [[CrossRef](#)]
38. Gupta, N.; Mahur, B.K.; Izrayeel, A.M.D.; Ahuja, A.; Rastogi, V.K. Biomass conversion of agricultural waste residues for different applications: A comprehensive review. *Environ. Sci. Pollut. Res.* **2022**, *29*, 73622–73647. [[CrossRef](#)]
39. EN ISO 18122:2016; Standard Solid Biofuels—Determination of ash Content. Available online: <https://sklep.pkn.pl/pn-en-iso-18122-2016-01p.html> (accessed on 28 November 2022).
40. ASTM D1622-03; Standard Test Method for Apparent Density of Rigid Cellular Plastics. Available online: <https://www.astm.org/d1622-03.html> (accessed on 28 November 2022).
41. Trovati, G.; Sanches, E.A.; Neto, S.C.; Mascarenhas, Y.P.; Chierice, G.O. Characterization of polyurethane resins by FTIR, TGA, and XRD. *J. Appl. Polym. Sci.* **2010**, *115*, 263–268. [[CrossRef](#)]
42. Gujral, P.; Varshney, S.; Dhawan, S. Designing of multiphase fly ash/MWCNT/PU composite sheet against electromagnetic environmental pollution. *J. Electron. Mater.* **2016**, *45*, 3142–3148. [[CrossRef](#)]
43. Kalemkiwicz, J.; Galas, D.; Sitarz-Palczak, E. The physicochemical properties and composition of biomass ash and evaluating directions of its applications. *Pol. J. Environ. Stud.* **2018**, *27*, 6. [[CrossRef](#)]
44. Vaiciukynienė, D.; Nizeviciene, D.; Kantautas, A.; Kiele, A.; Bocullo, V. Alkali activated binders based on biomass bottom ash and silica by-product blends. *Waste Biomass Valorization* **2021**, *12*, 1095–1105. [[CrossRef](#)]
45. Skevi, L.; Baki, V.A.; Feng, Y.; Valderrabano, M.; Ke, X. Biomass bottom ash as supplementary cementitious material: The effect of mechanochemical pre-treatment and mineral carbonation. *Materials* **2022**, *15*, 8357. [[CrossRef](#)] [[PubMed](#)]
46. Trivedi, N.S.; Mandavgane, S.A.; Mehetre, S.; Kulkarni, B.D. Characterization and valorization of biomass ashes. *Environ. Sci. Pollut. Res.* **2016**, *23*, 20243–20256. [[CrossRef](#)]
47. Ke, X.; Baki, V.A.; Skevi, L. Mechanochemical activation for improving the direct mineral carbonation efficiency and capacity of a timber biomass ash. *J. CO₂ Util.* **2023**, *68*, 102367. [[CrossRef](#)]
48. Yu, H.; Lei, Y.; Yu, X.; Wang, X.; Liu, T.; Luo, S. Batch foaming of carboxylated multiwalled carbon nanotube/poly(ether imide) nanocomposites: The influence of the carbon nanotube aspect ratio on the cellular morphology. *J. Appl. Polym. Sci.* **2015**, *132*, 42325. [[CrossRef](#)]
49. Yu, H.; Lei, Y.; Yu, X.; Wang, X.; Liu, T.; Luo, S. Solid-state polyetherimide (PEI) nanofoams: The influence of the compatibility of nucleation agent on the cellular morphology. *J. Polym. Res.* **2016**, *23*, 121. [[CrossRef](#)]
50. Pérez-Tamarit, S.; Solórzano, E.; Mokso, R.; Rodríguez-Perez, M.A. In-situ understanding of pore nucleation and growth in polyurethane foams by using real-time synchrotron X-ray tomography. *Polymer* **2019**, *166*, 50–54. [[CrossRef](#)]
51. Usta, N. Investigation of fire behavior of rigid polyurethane foams containing fly ash and intumescent flame retardant by using a cone calorimeter. *J. Appl. Polym. Sci.* **2012**, *124*, 3372–3382. [[CrossRef](#)]

52. Tarakçılar, A.R. The effects of intumescent flame retardant including ammonium polyphosphate/pentaerythritol and fly ash fillers on the physicomechanical properties of rigid polyurethane foams. *J. Appl. Polym. Sci.* **2011**, *120*, 2095–2102. [[CrossRef](#)]
53. Cao, X.; Lee, L.J.; Widya, T.; Macosko, C. Polyurethane/clay nanocomposites foams: Processing, structure and properties. *Polymer* **2005**, *46*, 775–783. [[CrossRef](#)]
54. Madaleno, L.; Pyrz, R.; Crosky, A.; Jensen, L.R.; Rauhe, J.C.M.; Dolomanova, V.; de Barros, A.M.M.V.; Pinto, J.J.C.; Norman, J. Processing and characterization of polyurethane nanocomposite foam reinforced with montmorillonite–carbon nanotube hybrids. *Compos. Part A* **2013**, *44*, 1–7. [[CrossRef](#)]
55. Paciorek-Sadowska, J.; Czupryński, B.; Borowicz, M.; Liszkowska, J. Rigid polyurethane–polyisocyanurate foams modified with grain fraction of fly ashes. *J. Cell. Plast.* **2020**, *56*, 53–72. [[CrossRef](#)]
56. Strakowska, A.; Członka, S.; Miedzińska, K.; Strzelec, K. Rigid polyurethane foams with antibacterial properties modified with pine oil. *Polimery* **2020**, *65*, 691–697. [[CrossRef](#)]
57. Shi, H.; Shi, D.; Yin, L.; Yang, Z.; Luan, S.; Gao, J.; Zha, J.; Yin, J.; Li, R.K. Ultrasonication assisted preparation of carbonaceous nanoparticles modified polyurethane foam with good conductivity and high oil absorption properties. *Nanoscale* **2014**, *6*, 13748–13753. [[CrossRef](#)] [[PubMed](#)]
58. Ng, Z.C.; Roslan, R.A.; Lau, W.J.; Gursoy, M.; Karaman, M.; Jullok, N.; Ismail, A.F. A green approach to modify surface properties of polyurethane foam for enhanced oil absorption. *Polymers* **2020**, *12*, 1883. [[CrossRef](#)] [[PubMed](#)]
59. Huang, P.; Wu, F.; Shen, B.; Zheng, H.; Ren, Q.; Luo, H.; Zheng, W. Biomimetic porous polypropylene foams with special wettability properties. *Compos. Part B* **2020**, *190*, 107927. [[CrossRef](#)]
60. Li, H.; Lin, S.; Feng, X.; Pan, Q. Preparation of superhydrophobic and superoleophilic polyurethane foam for oil spill cleanup. *J. Macromol. Sci. Part A Pure Appl. Chem.* **2021**, *58*, 758–768. [[CrossRef](#)]

Disclaimer/Publisher’s Note: The statements, opinions and data contained in all publications are solely those of the individual author(s) and contributor(s) and not of MDPI and/or the editor(s). MDPI and/or the editor(s) disclaim responsibility for any injury to people or property resulting from any ideas, methods, instructions or products referred to in the content.